Kinetic Analysis of Amyloid Protofibril Dissociation and Volumetric Properties of the Transition State

Abdul Raziq Abdul Latif,* Ryohei Kono,* Hideki Tachibana,† and Kazuyuki Akasaka*
*Department of Biotechnological Science, School of Biology-Oriented Science and Technology, Kinki University, Wakayama, Japan; and †Department of Biology, Faculty of Science, Kobe University, Kobe, Japan

ABSTRACT We present here the first detailed kinetic analysis of the dissociation reaction of amyloid protofibrils by utilizing pressure as an accelerator of the reaction. The experiment is carried out on an excessively diluted typical protofibril solution formed from an intrinsically denatured disulfide-deficient variant of hen lysozyme with Trp fluorescence as the reporter in the pressure range 3–400 MPa. From the analysis of the time-dependent fluorescence decay and the length distribution of the protofibrils measured on atomic force microscopy, we conclude that the protofibril grows or decays by attachment or detachment of a monomer at one end of the protofibril with a monomer dissociation rate independent of the length of the fibril. Furthermore, we find that the dissociation reaction is strongly dependent on pressure, characterized with a negative activation volume $\Delta V^{o\ddagger} = -50.5 \pm 1.60$ ml mol^{-1} at 0.1 MPa and with a negative activation compressibility $\Delta\kappa^{\ddagger} = -0.013 \pm 0.001$ ml mol^{-1} bar^{-1} or -0.9×10^{-6} ml g^{-1} bar^{-1}. These results indicate that the protofibril is a highly compressible high-volume state, but that it becomes less compressible and less voluminous in the transition state, most probably due to partial hydration of the existing voids. The system eventually reaches the lowest-volume state with full hydration of the monomer in the dissociated state.

INTRODUCTION

Amyloidosis is a class of diseases related to formation of amyloid fibrils from a number of proteins that, when folded, are often essential for cell function (1,2). Generally, the formation of amyloid fibrils in tissues is considered to be an extremely slow and complex process beyond the normal experimental reach of kinetic analysis based on the usual theory of chemical reaction. However, recent reports using a variety of techniques, particularly pressure, indicate that at least part of the process is reversible (3–6). Because delineation of the detailed molecular mechanisms of dissociation of amyloid fibrils would be crucial not only for advancing the basic understanding of amyloidosis but also for devising a means of its prevention, we have developed variable pressure experiments to probe the kinetics of fibril dissociation.

We report here the first detailed kinetic analysis of amyloid fibril dissociation reaction based on principles of chemical reaction rate theory. The analysis is made possible by employing a simple reaction system in which the concentration of the reactant and/or the product (fibrils) is followed quantitatively during the course of the reaction. It is commonly agreed that an amyloid fibril consists of a bundle of several protofilaments or protofibrils, each of which is a linear array of polypeptide chains rich in β-sheet, making the protofibril formation a crucial step in formation of amyloid fibrils. We focus on protofibril dissociation kinetics using a genetically engineered disulfide-deficient variant of hen lysozyme (0SS), with all eight cysteinyl residues replaced by alanine or serine. 0SS was chosen because, first, because the molecules are intrinsically unfolded with highly diminished secondary structure under conditions of no salt (7), but spontaneously form protofibrils in a mildly acidic solution at high ionic strength (8,9) (cf. Fig. 1 of Kamatari et al. (9)). Second, the dissociation reaction of the protofibril is greatly accelerated by increased pressure within a few kbar range, enabling direct spectroscopic (e.g., ^{1}H NMR) observation of the time dependence of the reaction (9). The pressure dependence of the dissociation rate is expected to give important volumetric information on the transition state structure for the first time for amyloid fibrils.

Pressure-jump fluorescence methods are used here to monitor the dissociation process selectively after excessively diluting the solution containing matured protofibrils of 0SS just before the jump. The excessive (~270-fold) dilution practically eliminates the reassociation reaction, allowing focus strictly on the dissociation reaction. The protein has six Trp residues, distributed throughout the molecule at residues 28, 62, 63, 108, 111, and 123; their strong fluorescence intensity provides a sensitive reporter of the dissociation reaction. The matured protofibrils are prepared by incubating monomeric 0SS (8 mg ml^{-1}) for 6–8 months in 20 mM sodium acetate buffer, pH 4.0, containing 30 mM NaCl at 25°C. Atomic force microscopy (AFM) is used to monitor the length-distribution of protofibrils, which gives a crucial test of the polymerization mechanism. Dissociation kinetic analysis is carried out based on the extension of the theory of linear polymerization reaction of proteins (monomer addition to a growing end) by Oosawa and Asakura (10), giving the intrinsic rate constant for the elementary reaction of a monomer dissociation from one end of the protofibril over a

Submitted May 5, 2006, and accepted for publication August 31, 2006.

Address reprint requests to Kazuyuki Akasaka, E-mail: akasaka8@spring8.or.jp.

0006-3495/07/01/323/07 $2.00

doi: 10.1529/biophysj.106.088120

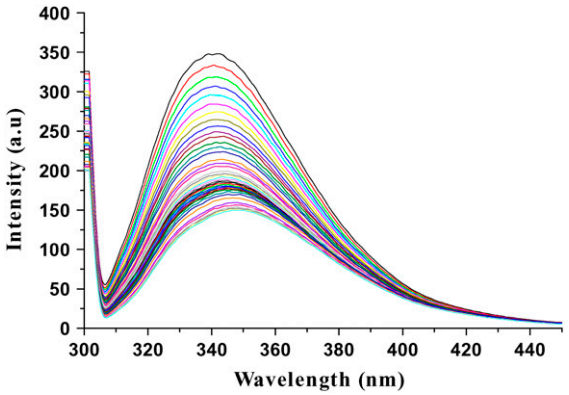

FIGURE 1 Pressure-induced changes of Trp fluorescencce spectrum of matured protofibrils of the disulfide-deficient hen lysozyme (0SS) at 350 MPa at 25°C. The protofibril solution (8 mg ml^{-1}) had been prepared by incubating the lyophilized 0SS sample in 20 mM sodium acetate buffer, 30 mM sodium chloride (pH 4.0) for 8 months and was diluted to 30 μg ml^{-1} in the same buffer just before applying pressure. The top spectrum was measured at 10 min after the pressure jump and the subsequent spectra were measured at 2-min intervals until the bottom spectrum was obtained at 240 min. Note the shift of the maximum emission from 338 to 350 nm concomitant with the decrease in intensity.

wide range of pressure (3–400 MPa). The results provide crucial volumetric information on the transition state of the protofibril dissociation for the first time.

MATERIALS AND METHODS

Preparation of matured protofibrils of 0SS

A genetically engineered disulfide-deficient variant of hen lysozyme 0SS, in which eight Cys residues are replaced by Ala or Ser was produced in *Escherichia coli*, and purified as described in Tachibana (7). To avoid precipitation, freeze-dried 0SS powder was first dissolved in pure water. Then the solution was mixed with sodium acetate buffer and sodium chloride solution to give a final protein concentration of 8 mg ml^{-1} in 20 mM sodium acetate buffer containing 30 mM sodium chloride, pH 4.0, and the association reaction started immediately (9). The progress of the reaction was monitored by circular dichroism (CD) (JASCO J-820) and AFM. The matured protofibrils were obtained by allowing the reaction to proceed for a sufficiently long time (6–8 months) at 25°C.

Atomic force microscopy

For obtaining AFM images of protofibrils, an aliquot of protofibril solution was deposited on mica surface and washed with pure water. AFM images were recorded with the cyclic contact mode at a frequency of 119 kHz on SPI-3800 (Seiko Instruments, Chiba, Japan).

High-pressure fluorescence measurements

The protofibril solution incubated for more than 6 months was diluted by ~270-fold into the final protein concentration of 30 μg mol^{-1} (2.1 μM), and immediately transferred into an optical cell of ~300 μl capacity in a high-pressure optical chamber (Teramecs, Kyoto, Japan) placed in a fluorescence spectrophotometer (Shimadzu RF-5300PC). For each experiment, pressure was adjusted (jumped) to a fixed value between 3 and 400 MPa with a hand pump (model TP-500/200; Teramecs), and the first measurement was made at ~10 min after the dilution and then continued up to several hours at 25°C at that pressure. For excitation, a 150 W xenon lamp was used at an excitation wavelength of 295 nm with a band width of 3 nm, while the fluorescence was detected with a band width of 10 nm.

Analysis of the fluorescence data

The time dependence of the fluorescence intensity from the amyloid protofibrils of 0SS was fitted with an exponential decay function of time, where the observed rate constant (k_{obs}) is related to the fluorescence intensity I at time t by the expression:

$$(I - I^{\infty})/(I^{o} - I^{\infty}) = \exp(-k_{obs} \times t)$$
$$\text{or} \quad \ln((I - I^{\infty})/(I^{o} - I^{\infty})) = -k_{obs} \times t, \qquad (1)$$

where I^{o} and I^{∞} are the intensities at time 0 and at time infinity, respectively. In this experiment, I^{∞} pertaining to the full dissociation, was determined experimentally after each experiment by bringing the pressure to 400 MPa for 10~30 min to attain complete dissociation, while I^{o} was determined by least-squares fit of the data to Eq. 1.

Analysis of pressure-dependent kinetics

The dissociation reaction of 0SS is considered to proceed through a transition state whose Gibbs energy is higher than that of the protofibril state by $\Delta G^{\ddagger}$, which would vary with pressure according to the equation expressed to the second-order in pressure P by

$$\Delta G^{\ddagger} = \Delta G^{o\ddagger} + \Delta V^{o\ddagger}(P - P^{o}) - (\Delta\kappa^{\ddagger}/2)(P - P^{o})^{2}, \quad (2)$$

where $\Delta G^{o\ddagger}$ refers to the Gibbs energy difference at 0.1 MPa, $\Delta V^{o\ddagger}$ the activation volume at 0.1 MPa, and $\Delta\kappa^{\ddagger}$ the activation compressibility, meaning the change in isothermal compressibility on activation or equivalently the pressure dependence of the activation volume. Then, the rate constant (k) is given by

$$k = (kT/h)\exp(-\Delta G^{\ddagger}/RT)$$
$$= (kT/h)\exp(-(\Delta G^{o\ddagger} + \Delta V^{o\ddagger}(P - P^{o}) - (\Delta\kappa^{\ddagger}/2)(P - P^{o})^{2})/RT)$$

or

$$\ln k = \ln(kT/h) - \Delta G^{o\ddagger}/RT - (\Delta V^{o\ddagger}/RT)(P - P^{o}) + (\Delta\kappa^{\ddagger}/2RT)(P - P^{o})^{2} \qquad (3)$$

and

$$(\partial(\ln k)/\partial P)_{T} = -(\Delta V^{o\ddagger}/RT) + (\Delta\kappa^{\ddagger}/RT)(P - P^{o})$$
$$\Delta V^{\ddagger} = \Delta V^{o\ddagger} - \Delta\kappa^{\ddagger}(P - P^{o})$$
$$\Delta\kappa^{\ddagger} = -(\partial\Delta V^{\ddagger}/\partial P)_{T},$$

where $\Delta V^{\ddagger}$ is the activation volume at pressure P, $\Delta V^{o\ddagger}$ is the activation volume at 0.1 MPa, and $\Delta\kappa^{\ddagger}$ is the change in activation volume with pressure. R is the universal gas constant and T is the absolute temperature. The values of $\Delta V^{o\ddagger}$ and $\Delta\kappa^{\ddagger}$ were determined by least-squares fitting of the experimentally obtained ln k versus P data (Fig. 4) to Eq. 3.

RESULTS AND DISCUSSION

Pressure-induced dissociation of 0SS protofibrils monitored by Trp fluorescence

Upon ~270-fold dilution of mature protofibrils (8 mg ml^{-1}) (see Materials and Methods for preparation) to a final

concentration of 30 μg ml^{-1} (2.1 μM) in 20 mM sodium acetate, 30 mM NaCl, pH 4.0, no spectral change takes place at 1 bar in a measurable time range, although the protofibrils should be fully dissociated in equilibrium under such a dilute condition. A strong Trp fluorescence emission was found with a maximum wavelength of ~338 nm, highly blue-shifted from >350 nm typical for an exposed Trp residue, indicating that in the protofibril state most of the six Trp residues are buried in nonpolar environments, well shielded from the solvent water.

When pressure is increased above ~50 MPa, the fluorescence spectrum decreases at a measurable rate, with a final intensity of about half the starting intensity (Fig. 1). Along with a decrease in intensity, there is a distinct shift of the wavelength of maximum emission from the initial value of ~338 nm to a final value of ~350 nm, indicating that initially buried Trp residues become exposed to aqueous solvent at high pressure. Pressure dissociation into monomeric species has been confirmed in previous NMR experiments (8,9). The fluorescence spectrum shows no appreciable change when the pressure is returned to 3 MPa, indicating that the pressure-induced dissociation is irreversible under the excessive dilution, in contrast to the full reversibility of the dissociation reaction for the case of no dilution (9).

Because the 0SS protofibril consists predominantly of β-sheet structure (8), each Trp residue is most likely buried between β-strands, either intermolecularly or intramolecularly. Along with the previous NMR observation that the Trp residues are likely to act as initial association sites in formation of the protofibril (8), this observation suggests the importance of hydrophobic interactions of Trp residues in the association of protofibrils. In accordance with this, we found that the quantum yield of Trp fluorescence in 0SS protofibrils is unusually high. The fluorescence quantum yield of wild-type hen lysozyme is considerably lower ($Q = 0.0707$), because only Trp-62 and Trp-108 are dominant (80% of total) emitters of the fluorescence (11). The relative Trp fluorescence intensities among wild-type hen lysozyme, 0SS monomer, and 0SS protofibril are 1.0, 1.79, and 3.43, respectively (data not shown). The quantum yield of 0SS in the fibrillar state is given approximately by $Q = 0.0707 \times 3.43 = 0.243$. The high quantum yield and the blue-shifted of the emission to 338 nm of the Trp fluorescence suggest strongly that all the six Trp residues of the protofibril are in a hydrophobic environment. Since the six Trp residues are distributed over the entire 0SS molecule at positions 28, 62, 63, 108, 111, and 123, this suggests that a major part of the polypeptide chain is involved in stabilizing interactions in the 0SS protofibril.

Fig. 2 plots the logarithm of normalized fluorescence intensity ln $((I - I^{\infty}) / (I^{o} - I^{\infty}))$ at 338 nm against time, where I, I^{∞}, and I^{o} are the intensity at time t, at infinite time, and at time 0, respectively. The intensity change, at least up to 70 min, clearly follows a single-exponential function of time, giving an apparent rate constant k_{obs} at each pressure (cf. Eq. 1). The single-exponential decay is not a trivial

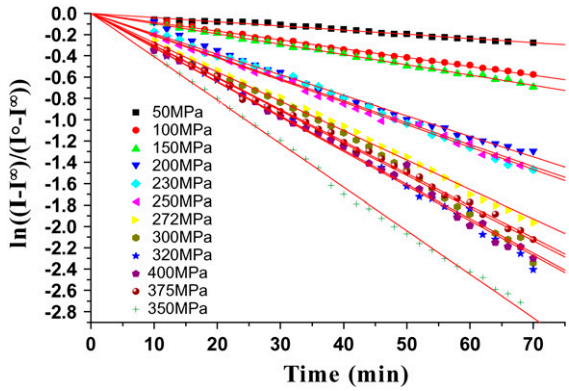

FIGURE 2 Plot of the logarithm of normalized fluorescence intensity, ln $((I - I^{\infty}) / (I^{o} - I^{\infty}))$, at 338 nm against time at a constant pressure between 50 and 400 MPa at 25°C (Data taken from Fig. 1). The straight lines are best-fit of the data points to Eq. 1, the slope giving apparent dissociation rate constant (k_{obs}) at respective pressures.

observation, considering that our system should be a heterogeneous size mixture of protofibrils, which potentially have different rates of dissociation. The single-exponential decay is a consequence of the particular mechanism governing the protofibril formation and dissociation, as shown below.

Length distribution of protofibrils and the reaction scheme: linear-polymerization

High-pressure NMR experiments demonstrate that the pressure-dependent association and dissociation of 0SS molecules is clearly reversible (8,9). The pressure-jump ^{1}H NMR study suggested, as a major mechanism of 0SS association and dissociation, a linear-polymerization reaction for addition of monomers, which may be expressed by the reaction scheme

$$\text{Protofibril}\ (\text{n}-\text{mer}) \underset{(k_+)}{\overset{(k_-)}{\rightleftarrows}} \text{Protofibril}\ (\text{n}-1\ \text{mer}) + \text{monomer} \qquad \text{(Scheme 1)}$$

in which k_+ and k_- represent, respectively, the intrinsic rate constants for association and dissociation of monomer at one end of a polymer; they are defined as parameters independent of polymer length (9). In this mechanism, the equilibrium concentration of the polymer composed of i monomeric units, C_i, is expressed by an exponential-type function of i (10):

$$C_i \propto r^{i-1} (0 < r < 1). \qquad (4)$$

Fig. 3 shows in histograms the length distribution of protofibrils in the starting material, i.e., the mature 0SS protofibrils incubated for 6 months, obtained by actually ''measuring'' the length of each protofibril in the AFM image over a sufficient number of protofibrils. We found that the population C_l decreases with length l, which was fitted well with an exponential function (the *solid curve* in Fig. 3)

$$C_l \propto \exp(-l/394). \qquad (5)$$

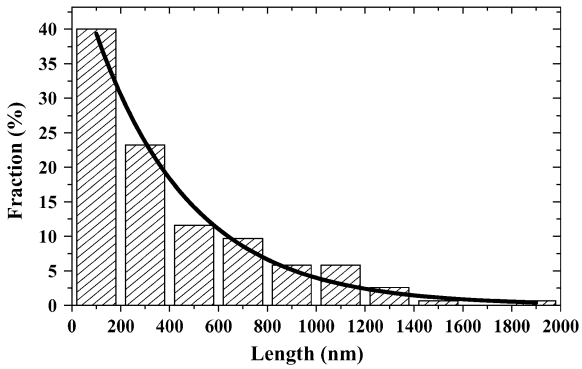

FIGURE 3 Histogram of the length distribution of amyloid protofibrils of the disulfide-deficient hen lysozyme. The protofibril solution (8 mg ml^{-1}) had been prepared by incubating the lyophilized 0SS in 20 mM sodium acetate buffer, 30 mM sodium chloride, pH 4.0, for 8 months. The length of each protofibril was measured on the atomic force microscopy image over a sufficient number of protofibril fibers. The solid line is a fit of the experimentally determined population C_l of the fibril of length l (nm) with an exponential function of length l, giving $C_l \propto \exp(-l/394)$.

Assuming that an 0SS monomeric unit spans l_0 nm along the fibril axis, the number of monomeric units in the polymer is given by $i = l/l_0$, Eq. 5 is transformed into

$$C_i \propto (\exp(-i\,l_0/394)) \propto (\exp(-l_0/394))^{i-1}.$$

This conforms to Eq. 4 with the r-value of $\exp(-l_0/394)$. Note that the equilibrium concentration of the polymer consisting of i monomeric units decreases exponentially with increasing i, in agreement with the observation in Fig. 3. Thus Scheme 1, a linear-polymerization reaction for addition of monomer, is likely to be the major mechanism of growth and shrinkage of 0SS protofibrils.

It is noted here that observations of elongation of single amyloid fibers have indicated as a dominant mechanism of association either bidirectional (elongation from both ends) (12–14) or unidirectional (elongation from one end) (15,16) elongation mechanism. By analogy with the well-known example of the distinction between plus and minus ends of actin or tubulin filaments and from the reasoning of equilibrium between association and dissociation, it follows that the dissociation reaction is also expected to occur, correspondingly, bidirectionally or unidirectionally. At present, however, we have no information about the polarity of association or that of dissociation of 0SS fibrils. Therefore, for simplicity, we assumed that the dissociation takes place from one end. If dissociation occurs equally from both ends, the estimation of the intrinsic dissociation rate constant described below will simply be half as much as the rate obtained for the case of the dissociation from one end.

The intrinsic dissociation rate of the monomer

If the number concentration of the polymer obeys an exponential-type distribution before the start of the dissociation, $C_i\,(t=0) \propto r^{i-1}$, and if the dissociation of the monomer occurs from the polymer end with an intrinsic dissociation rate constant k_-, then, during the dissociation reaction the total concentration of polymers C_p (expressed in the total concentration of monomeric units incorporated into polymers) should also decrease exponentially with time. In this case,

$$C_p = C_p(0)\exp(-k_-(1-r)t). \quad (6)$$

(See Supplementary Material for the derivation of Eq. 6). Accordingly, a normalized fluorescence intensity $(I - I^\infty)/(I^0 - I^\infty)$ should also decrease exponentially with time,

$$(I - I^\infty)/(I^0 - I^\infty) = \exp(-k_-(1-r)t), \quad (7)$$

with an apparent rate constant

$$k_{obs} = k_-(1-r).$$

Equation 7 predicts a single-exponential decay of the fluorescence intensity with time, which is exactly what is experimentally observed (Fig. 2). Note that this coincidence is not a trivial outcome of first-order dissociation, but an outcome of Scheme 1, a linear-polymerization mechanism (see Supplementary Material for more details).

From pressure-jump NMR experiments (9), end-to-end polymer association and splitting was suggested as a mechanism in addition to linear polymerization. A polymer splitting reaction would not be detected directly in this experiment, because such a reaction would not cause significant change in Trp fluorescence. However, if this should occur frequently, it would be expected to change the length distribution appreciably and to affect the decay profile of fluorescence with time. This being unnoticed in Fig. 2, such a reaction is apparently much less frequent than is consistent with Scheme 1, at least in the first ~70 min of the reaction.

For l_0, the unit length of the protofibril along the fibril axis, we have no direct information at present. We assume what we consider a reasonable value for the unit length. The molar volume of 0SS, 10,010 ml mol^{-1} (based on its *M*r and partial specific volume), corresponds to a molecular volume (V_m), 16.6 nm^3, of a 0SS monomeric unit. On the other hand, there exists uncertainty about the diameter of the fibril; whereas it was ~2 nm from AFM observation (9), our preliminary small-angle x-ray scattering measurement (R. Kono, T. Fujisawa, H. Tachibana, and K. Akasaka, unpublished data) shows that it is as much as 4 nm or even larger. As a compromise, we assume a diameter of 3 nm, which gives the volume (V_f) of 7.07 nm^3 for a fibril segment of a unit length (=1 nm) along the fibril axis. The corresponding l_0 ($=V_m/V_f$) is 2.35 nm, which is simplified here to be 2 nm. Then the number concentration of the protofibril that consists of i monomeric units is expressed by $C_i \propto r^{i-1} = \exp(-i/197)$, where $r = \exp(-1/197) = 0.995$. This gives the intrinsic dissociation rate constant $k_- = k_{obs}/(1-r) \sim 200\,k_{obs}$. The intrinsic dissociation rate constant should be ~200 times larger than the observed (apparent) dissociation rate constant. For example, if the observed rate is 0.0157 min^{-1} at 200 MPa, then the intrinsic rate of the monomer dissociation

should be $k_- \sim 200 \times 0.0157\ \text{min}^{-1} = 3.1\ \text{min}^{-1}$. Thus, the dissociation takes place, on average, once for every ~20 s. (When the uncertainty about the fibril diameter is taken into consideration, this value ranges from 4 to 50 s.)

The volumetric properties of the fibril and the transition states

Dissociation of mature protofibrils of 0SS is immeasurably slow just by dilution, apparently prohibited by a relatively large activation free energy ($\Delta G^{o\ddagger}$) in Eq. 2. Pressure dramatically accelerates dissociation. For example, $k_{obs} = 0.0020\ \text{min}^{-1}$ at 50 MPa increases to $0.0157\ \text{min}^{-1}$ at 200 MPa and to $0.0354\ \text{min}^{-1}$ at 400 MPa. Qualitatively, this means that the positive $\Delta G^{o\ddagger}$ barrier is compensated by a negative contribution from $\Delta V^{o\ddagger}(P - P^o) - (\Delta\kappa^{\ddagger}/2)(P - P^o)^2$ terms in Eq. 2. The experiments also allow us to determine values for the important parameters, $\Delta V^{o\ddagger}$ and $\Delta\kappa^{\ddagger}$, as described below.

Fig. 4 shows the plot of the logarithm of k_{obs} against pressure in range 3–400 MPa. Note that ln k_{obs} increases almost linearly at low pressure, but becomes distinctly nonlinear above ~200 MPa, reaching a plateau around 350~400 MPa. Following Eq.3, the linear increase of ln k_{obs} in the low-pressure range indicates that the activation volume, $\Delta V^{0\ddagger} = V^0$ (transition state) $- V^0$ (protofibril state), is negative. Leveling off of the increase in the high-pressure range indicates that the compressibility of activation (or the pressure dependence of the activation volume, $\Delta\kappa^{\ddagger} = \kappa$ (transition state) $- \kappa$ (protofibril state) $= -\partial\Delta V^{0\ddagger}/\partial P$, is also negative. Fits of the data to Eq. 3 give the activation volume and the compressibility change. $\Delta V^{0\ddagger} = -50.5 \pm 1.6$ ml·mol monomer^{-1}. $\Delta\kappa^{\ddagger} = -0.013 \pm 0.0007$ ml mol monomer^{-1} bar^{-1} (1 bar = 0.1 MPa).

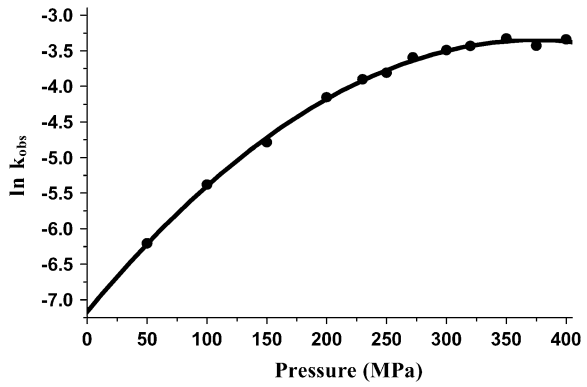

FIGURE 4 Plot of logarithm of observed dissociation rate (k_{obs}) (obtained from Fig. 2) against pressure. The original solution of 0SS protofibrils (8 mg ml^{-1}) was excessively diluted to 30 μg ml^{-1} in 20 mM sodium acetate buffer, 30 mM sodium chloride (pH 4.0) just before applying pressure for irreversible dissociation at 25°C. The solid line represents the least-squares fit of the experimental data to Eq. 3, giving $\Delta V^{0\ddagger} = -50.5 \pm 1.6$ ml mol monomer^{-1} and $\Delta\kappa^{\ddagger} = -0.013 \pm 0.0007$ ml mol monomer^{-1} bar^{-1} (1 bar = 0.1 MPa). Extrapolation of the curve to 0.1 MPa gives $k_{obs} = 0.000773\ \text{min}^{-1}$ or $\tau = 1290$ min or 21.6 h.

The negative activation volume $\Delta V^{0\ddagger} = -50.5 \pm 1.6$ ml·mol monomer^{-1} indicates that the partial molar volume V^0 of 0SS in the protofibril state decreases considerably in the transition state for dissociation. A decrease in partial molar volume is generally associated with hydration of the protein molecule, in particular the hydration of cavities or voids and the electrostriction of water surrounding charged residues. The large negative $\Delta V^{0\ddagger}$ observed would imply that considerable hydration takes place in the transition state for dissociation in the dissociation end of the protofibril. Alternately, this could mean that the protofibril state is a relatively high volume state.

We have no direct measurement of ΔV^0 for dissociation of the mature protofibrils, which is obviously quite difficult because it may take several months for each equilibration reaction, but we previously measured it for younger protofibrils of 0SS grown in ~1 day (8). (We recently confirmed the formation of shorter protofibrils in ~1 day incubation by AFM.) The ΔV^0 value should not be different between the young and the mature protoribrils as long as Scheme 1 applies, because only the volume change in the dissociating end of the polymer counts and this should be nearly the same for the two cases. In a previous publication (8), an equilibrium volume change ΔV of -52.7 ± 11.3 ml mol monomer^{-1} (as average over for 3–200 MPa by assuming $\Delta\kappa = 0$) was determined by assuming the highly cooperative reaction scheme,

$$\text{Protofibril (n - mer)} \quad \rightleftarrows \quad \text{n monomers.} \qquad \text{(Scheme 2)}$$

Now that we know Scheme 1 fits the reality, we have recalculated ΔV using the same data for Scheme 1. We obtain $\Delta V = -100 \pm 9$ ml mol monomer^{-1} (as average over for 3–200 MPa by assuming $\Delta\kappa = 0$), a relatively large negative value. By assuming that $\Delta V^0 \sim \Delta V \sim -100$ ml mol monomer^{-1}, a volume-pressure diagram is drawn in Fig. 5.

A decrease in the partial molar volume upon unfolding is commonly observed for globular proteins. The negative volume change ΔV^0 of $-20 \sim -100$ ml mol monomer^{-1} is usually obtained for 10–20 kD proteins (17), which is contributed mainly from hydration of cavities and electrostriction of water surrounding charged side chains. For hen lysozyme (wild-type), reported values of ΔV^0 for the transition from folded monomer to unfolded monomer are only $\Delta V^0 \sim -10 \sim -26$ ml mol^{-1} (23°C, pH 7.6) (18–21). Under the assumption that the effect of disulfide bonds on the volume of the denatured conformer is not too large, this would mean that the partial volume is larger in the protofibril state than in the folded native state, which generally is the largest volume state of a globular protein when no intermolecular association is present. Although the origin of this high volume of the protofibril state is not clear at present, a general view for the high-volume folded state of a globular protein is that its main contribution is cavities or voids often in the interior of the folded matrix. The unusually high quantum yield and the unusual blue shift of the emission maximum of the Trp fluorescence indicate that most of the

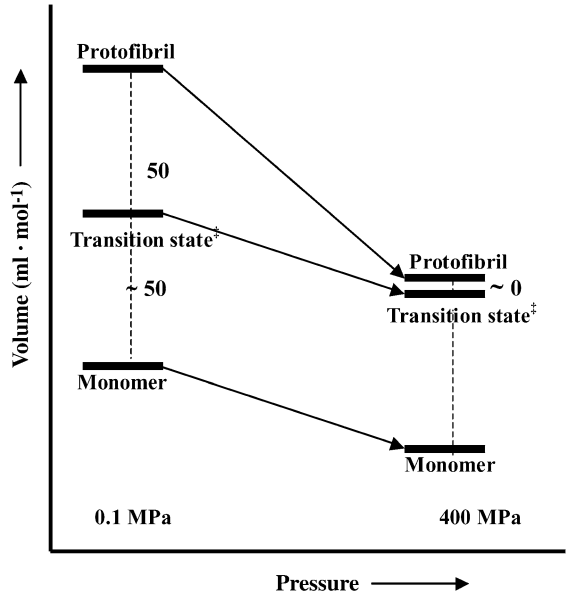

FIGURE 5 The volume diagram for 0SS in the dissociation reaction of amyloid protofibrils at 0.1 MPa and at 400 MPa at 25°C. At 0.1 MPa, the transition state is ~50 ml mol^{-1} below the protofibril state ($\Delta V^{\circ\ddagger} = -50.5 \pm 1.6$ ml·mol monomer^{-1}). However, this difference becomes almost null at 400 MPa because the compressibility is larger in the protofibril state than in the monomeric state ($\Delta\kappa^{\ddagger} < 0$). Note that the volume changes between 0.1 MPa and 400 MPa are unknown for both the protofibril and monomeric states so that the relative levels between the two pressures are arbitrarily drawn.

six Trp residues are buried in hydrophobic environment. This means that a large part of the polypeptide chain of 0SS is involved in intra- and intermolecular interactions in the prototibril state. Dissociation of the protofibril could result in a negative ΔV^0 value due to the collapse of cavities and contraction of water around freed charges in a large part of the polypeptide chain buried in the protofibril state.

The above view of loose packing with voids in the protofibril is compatible with a significant decrease in compressibility on activation ($\Delta\kappa^{\ddagger} = -0.013 \pm 0.001$ ml mol monomer^{-1} bar^{-1} or -0.9×10^{-6} ml g^{-1} bar^{-1}), meaning that the protofibril state is more compressible than the transition state, κ (protofibril state) $> \kappa$ (transition state). More specifically, because the dissociation of the protofibril takes place by detachment of a monomer from one end of the polymer, this difference in compressibility arises from the dissociating end of the protofibril. To our knowledge, there are no reports of $\Delta\kappa^{\ddagger}$ for dissociation in any other protofibrils or amyloid fibrils. Equilibrium changes in isothermal compressibility ($\Delta\kappa$) for unfolding of globular proteins, obtained from analysis of pressure-induced denaturation experiments, all report positive $\Delta\kappa$ values between 0.013 and 0.03 ml mol^{-1} bar^{-1} (22–25), i.e., the compressibility increases upon pressure denaturation.

The negative value of $\Delta\kappa^{\ddagger}$ could be a unique property of protofibril dissociation, which is likely to originate from a uniquely high compressibility in the protofibril state. On the other hand, Chalikian et al. (26,27) found that when compressibility is measured directly on folded and unfolded proteins at 1 bar by ultrasonic velocity measurements, the change in isothermal compressibility $\Delta\kappa^{\ddagger}$ can be positive or negative, depending on the state of denaturation. Native-to-compact intermediate transitions are accompanied by increase in κ ($\Delta\kappa = (1\text{–}4) \times 10^{-6}$ cm^{3}g^{-1}bar^{-1}), but native-to-partially unfolded transitions are accompanied by decrease in κ ($\Delta\kappa = -(3\text{–}7) \times 10^{-6}$ cm^{3}g^{-1}bar^{-1}), and native-to-fully unfolded transitions are accompanied by even larger decrease in κ ($\Delta\kappa = -(18\text{–}20) \times 10^{-6}$ cm^{3}g^{-1}bar^{-1}). Thus, the negative value of $\Delta\kappa^{\ddagger}$ could also be attributed to partial exposure of buried residues to water in the transition state, fully consistent with the partial hydration view from the large negative ΔV value. It should be noted that although the sign of the recently reported $\Delta\kappa^{\ddagger}$ for unfolding of apocytochrome b_{562} mutant is difficult to be established due to insufficient accuracy of the data as the authors state (28), the negative activation volume observed for the unfolding indicates significant hydration in its transition state ensemble in accord with the present finding.

Fig. 5 depicts a summary diagram of volume as a function of pressure obtained from these experiments. The protofibril state, in which most of the polypeptide chain is involved in intra- and intermolecular interactions, is a high-volume state, even higher than folded hen lysozyme. Regarding volume, the transition state ($\Delta V^{\ddagger} = -50.5 \pm 1.6$ ml mol^{-1}) is situated just halfway to the full dissociation at 0.1 MPa. The considerably large negative volume change in the transition state for protofibril dissociation suggests that considerable hydration takes place in the transition state, which according to Scheme 1 takes place at one end of the protofibril. Apparently, the protofibril at the dissociating end of the polymer occasionally fluctuates to a transition state having a higher degree of hydration. Interestingly, the difference in volume becomes almost null at ~400 MPa due to higher compression in the protofibril state, predicting that at still higher pressure (>400 MPa) the dissociation rate should start to decrease.

CONCLUSION

We have confirmed that the formation and dissociation of amyloid protofibrils of disulfide-deficient hen lysozyme (0SS) proceed largely by the linear polymerization mechanism with monomer attachment or detachment (Scheme 1). The fluorescence data suggest that the polypeptide chains of 0SS protofibrils are held together by hydrophobic interactions involving the six Trp residues beside the obvious interstrand hydrogen bonding and electrostatic interactions. The volumetric data suggest that the protofibril state is a highly compressible, high-volume state with considerable voids at least at its dissociable end and that in the transition state these voids are partially hydrated. The physicochemical origin of pressure-induced dissociation of the protofibrils has been disclosed by this work; the association-dissociation

equilibrium in protofibrils is driven toward dissociation by pressure because of a large decreasing volume upon dissociation, whereas the dissociation rate is increased by pressure because of a large negative volume of activation. The acceleration will be limited to a certain range of pressure, however, because the negative volume of activation may become null and eventually turn into positive at extremely high pressure, because of a decreased compressibility in the transition state. Generality of this conclusion for protofibrils other than 0SS is to be pursued in future studies. However, the experimental method and the analysis presented here are expected to be generally applicable for clarifying dissociation mechanisms and carrying out volumetric analysis of various protein assemblies including amyloidgenic and non-amyloidgenic aggregates.

SUPPLEMENTARY MATERIAL

An online supplement to this article can be found by visiting BJ Online at http://www.biophysj.org.

This work was carried out as an activity of the Japan Society for the Promotion of Science Core-to-Core Program–Integrated Action Initiative 17009.

A. Abdul Latif is grateful to JSPS for a postdoctoral fellowship for foreign researchers. Y.K. is a recipient of the COE fellowship of Kinki University from the Ministry of Education, Culture, Sports, Science and Technology (MEXT). This work was financially supported by Grants-in-Aid for Scientific Research Nos. 16370054 and 17570132 from MEXT and partly by the Bovine Spongiform Encephalopathy Control Project from the Ministry of Agriculture, Forestry and Fisheries.

REFERENCES

1. Dobson, C. M. 1999. Protein misfolding, evolution and disease. *Trends Biochem. Sci.* 24:329–332.
2. Koo, E. H., P. T. Lansbury, and J. W. Kelly. 1999. Amyloid disease; abnormal protein aggregation in neurodegeneration. *Proc. Natl. Acad. Sci. USA.* 96:9989–9990.
3. Dubois, J., A. A. Ismail, S. L. Chan, and Z. Ali-Khan. 1999. Fourier transform infrared spectroscopic investigation of temperature- and pressure-induced disaggregation of amyloid A. *Scand. J. Immunol.* 49:376–380.
4. Foguel, D., M. C. Suarez, A. D. Ferrao-Gonzales, T. C. Porto, L. Palmieri, C. M. Einsiedler, L. R. Andrade, H. A. Lashuel, P. T. Lansbury, J. W. Kelly, and J. L. Silva. 2003. Dissociation of amyloid fibrils of alpha-synuclein and transthyretin by pressure reveals their reversible nature and the formation of water-excluded cavities. *Proc. Natl. Acad. Sci. USA.* 100:9831–9836.
5. Seefeldt, M. B., J. Ouyang, W. A. Froland, J. F. Carpenter, and T. W. Randolph. 2004. High-pressure refolding of bikunin; efficacy and thermodynamics. *Protein Sci.* 13:2639–2650.
6. Carulla, N., G. L. Caddy, D. R. Hall, J. Zurdo, M. Gairi, M. Feliz, and E. Giralt. 2005. Molecular recycling within amyloid fibrils. *Nature.* 436:554–558.
7. Tachibana, H. 2000. Propensities for the formation of individual disulfide bonds in hen lysozyme and in the size and stability of disulfide-associated submolecular structure. *FEBS Lett.* 480:175–178.
8. Niraula, T. N., T. Konno, H. Li, H. Yamada, K. Akasaka, and H. Tachibana. 2004. Pressure-dissociable reversible assembly of intrinsically denatured lysozyme is a precursor for amyloid fibrils. *Proc. Natl. Acad. Sci. USA.* 101:4089–4093.
9. Kamatari, Y. O., S. Yokoyama, H. Tachibana, and K. Akasaka. 2005. Pressure-jump NMR study of dissociation and association of amyloid protofibrils. *J. Mol. Biol.* 349:916–921.
10. Oosawa, F., and S. Asakura. 1975. Thermodynamics of the Polymerization of Protein. Academic Press, London, UK.
11. Imoto, T., L. S. Forster, J. A. Rupley, and F. Tanaka. 1972. Fluorescence of lysozyme; emissions from tryptophan residues 62 and 108 and energy migration. *Proc. Natl. Acad. Sci. USA.* 69:1151–1155.
12. Goldsbury, C., J. Kistler, U. Aebi, T. Arvinte, and G. J. S. Cooper. 1999. Watching amyloid fibrils grow by time-lapse atomic force microscopy. *J. Mol. Biol.* 285:33–39.
13. Blackley, H. K. L., G. H. W. Sanders, M. C. Davies, C. J. Roberts, S. J. B. Tendler, and M. J. Wilkinson. 2000. *In-situ* atomic force microscopy study of β-amyloid fibrillization. *J. Mol. Biol.* 298:833–840.
14. Scheibel, T., A. S. Kowal, J. D. Bloom, and S. L. Lindquist. 2001. Bidirectional amyloid fiber growth for a yeast prion determinant. *Curr. Biol.* 11:366–369.
15. Inoue, Y., A. Kishimoto, J. Hirao, M. Yoshida, and H. Taguchi. 2001. Strong growth polarity of yeast prion fiber revealed by single fiber imaging. *J. Biol. Chem.* 276:35227–35230.
16. Ban, T., D. Hamada, K. Hasegawa, H. Naiki, and Y. Goto. 2003. Direct observation of amyloid fibril growth monitored by thioflavin T fluorescence. *J. Biol. Chem.* 278:16462–16465.
17. Royer, C. A. 2002. Revisiting volume changes in pressure-induced protein unfolding. *Biochim. Biophys. Acta.* 1595:201–209.
18. Zipp, A., and W. Kauzmann. 1973. Pressure denaturation of metmyoglobin. *Biochemistry.* 12:4217–4228.
19. Li, T. M., J. W. Hook, H. G. Drickamer, and G. Weber. 1976. Plurality of pressure-denatured forms in chymotrypsinogen and lysozyme. *Biochemistry.* 15:5571–5580.
20. Peng, X., J. Jonas, and J. L. Silva. 1993. Molten-globule conformation of Arc repressor monomers determined by high-pressure ^{1}H-NMR spectroscopy. *Proc. Natl. Acad. Sci. USA.* 90:1776–1780.
21. Samarasinghe, S. D., D. M. Campbell, and J. J. Jonas. 1992. High-resolution NMR study of the pressure-induced unfolding of lysozyme. *Biochemistry.* 31:7773–7778.
22. Hawley, S. A. 1971. Reversible pressure-temperature denaturation of chymotrypsinogen. *Biochemistry.* 10:2436–2442.
23. Prehoda, K. E., E. S. Moorberry, and J. L. Markley. 1998. Pressure denaturation of proteins: evaluation of compressibility effects. *Biochemistry.* 37:5785–5790.
24. Lassalle, M. W., H. Yamada, and K. Akasaka. 2000. The pressure-temperature free energy-landscape of staphylococcal nuclease monitored by 1H-NMR. *J. Mol. Biol.* 298:293–302.
25. Seemann, H., R. Winter, and C. A. Royer. 2001. Volume expansivity and isothermal compressibility changes associated with temperature and pressure unfolding of Staphylococcal nuclease. *J. Mol. Biol.* 307: 1091–1102.
26. Chalikian, T. V., and K. J. Breslauer. 1996. On volume changes accompanying conformational transitions of biopolymers. *Proc. Natl. Acad. Sci. USA.* 93:1012–1014.
27. Taulier, N., and T. V. Chalikian. 2002. Compressibility of protein transitions. *Biochim. Biophys. Acta.* 1595:48–70.
28. Korzhnev, D. M., I. Bezsonova, F. Evanics, N. Taulier, Z. Zhou, Y. Bai, T. V. Chalikian, R. S. Prosser, and L. E. Kay. 2006. Probing the transition state ensemble of a protein folding reaction by pressure-dependent NMR relaxation dispersion. *J. Am. Chem. Soc.* 128:5262–5269.